# Induced *Gnas*$^{R201H}$ expression from the endogenous *Gnas* locus causes fibrous dysplasia by up-regulating Wnt/β-catenin signaling

Sanjoy Kumar Khan[a], Prem Swaroop Yadav[a], Gene Elliott[b], Dorothy Zhang Hu[c], Ruoshi Xu[a,d], and Yingzi Yang[a,e,1]

[a]Department of Developmental Biology, Harvard School of Dental Medicine, Boston, MA 02115; [b]National Human Genome Research Institute, National Institutes of Health, Bethesda, MD 20892; [c]Department of Oral Medicine, Infection, and Immunity, Harvard School of Dental Medicine, Boston, MA 02115; [d]West China School of Stomatology, Sichuan University, Chengdu 610041, P. R. China; and [e]Harvard Stem Cell Institute, Cambridge, MA 02138

Edited by John T. Potts, Massachusetts General Hospital, Charlestown, MA, and approved October 23, 2017 (received for review August 15, 2017)

**Fibrous dysplasia (FD; Online Mendelian Inheritance in Man no. 174800) is a crippling skeletal disease caused by activating mutations of the *GNAS* gene, which encodes the stimulatory G protein Gα$_s$. FD can lead to severe adverse conditions such as bone deformity, fracture, and severe pain, leading to functional impairment and wheelchair confinement. So far there is no cure, as the underlying molecular and cellular mechanisms remain largely unknown and the lack of appropriate animal models has severely hampered FD research. Here we have investigated the cellular and molecular mechanisms underlying FD and tested its potential treatment by establishing a mouse model in which the human FD mutation (R201H) has been conditionally knocked into the corresponding mouse *Gnas* locus. We found that the germ-line FD mutant was embryonic lethal, and Cre-induced *Gnas* FD mutant expression in early osteochondral progenitors, osteoblast cells, or bone marrow stromal cells (BMSCs) recapitulated FD features. In addition, mosaic expression of FD mutant Gα$_s$ in BMSCs induced bone marrow fibrosis both cell autonomously and non-cell autonomously. Furthermore, Wnt/β-catenin signaling was up-regulated in FD mutant mouse bone and BMSCs undergoing osteogenic differentiation, as we have found in FD human tissue previously. Reduction of Wnt/β-catenin signaling by removing one *Lrp6* copy in an FD mutant line significantly rescued the phenotypes. We demonstrate that induced expression of the FD Gα$_s$ mutant from the mouse endogenous *Gnas* locus exhibits human FD phenotypes in vivo, and that inhibitors of Wnt/β-catenin signaling may be repurposed for treating FD and other bone diseases caused by Gα$_s$ activation.**

fibrous dysplasia | McCune–Albright syndrome | Gnas | Wnt/β-catenin | LGK-974

Fibrous dysplasia (FD) of bone (Online Mendelian Inheritance in Man no. 174800) is a severe form of skeletal disorder resulting in deformity, fracture, and pain in the affected bone. FD is well-characterized by bone marrow fibrosis; the bone marrow space is devoid of both hematopoietic tissue and adipocytes and replaced with fibrotic tissue. FD bone also exhibits abnormal architecture ("Chinese writing" pattern), structure, and mineral content of bone trabeculae (1–3). These complex changes result in a mechanically incompetent, brittle, and fracture-prone bone that can cause wheelchair confinement of severely affected individuals. FD is a rare skeletal genetic disorder caused by mosaic activating mutations (R201H or R201C) of the α-subunit of stimulatory G protein (Gα$_s$) encoded by *GNAS* (4–6). The activating mutant Gα$_s$ loses inherent GTPase activities and remains in a constitutively active form that stimulates excessive cAMP production (7). FD occurs in isolation or with other clinical features such as skin pigmentation and endocrine dysfunction in McCune–Albright syndrome (MAS) (8, 9). Lack of inheritance of FD/MAS (4, 5, 10, 11) is likely due to embryonic lethality caused by germ line-transmitted activating *GNAS* mutations, which can only survive through mosaicism (12).

There is no cure for FD, as the molecular and cellular mechanisms of this skeletal disease that can be devastating in some cases remain largely unknown. Mouse models are indispensable tools for elucidating the natural history of human diseases and designing and testing novel treatments. Better understanding of FD is essential to providing new insights into marrow fibrosis and the regulation of osteoblast differentiation and maturation from bone marrow stromal cells (BMSCs, also called bone marrow-derived stem cells), but the lack of appropriate animal models has severely hampered research advancement and therapeutic development for FD. The existing in vivo models are either based on xenotransplantation of *GNAS*-mutated human skeletal progenitor cells into immunocompromised mice (11) or transgenic mouse models in which either an engineered Gα$_s$-coupled receptor or a mutated rat *Gnas* transgene was driven by artificial promoters (13–15). As none of these models were able to accurately recapitulate pathophysiological characteristics of human FD, the development of a "knockin" (KI) mouse model in which the corresponding mouse mutant Gα$_s$ can be expressed from its endogenous locus is absolutely necessary.

Here we have successfully created a KI mouse line, *Gnas*$^{f(R201H)}$, in which the human FD mutation (R201H) has been conditionally "knocked into" the corresponding mouse *Gnas* locus to allow FD mutant *Gnas* expression from its endogenous genetic locus with temporal and tissue specificity upon Cre induction. Using this mouse line, we show that FD mutant *Gnas* expression in both osteochondral progenitor cells and osteoblast progenitor cells in the *Prrx1* and *Osx* lineages, respectively, replicated human FD

## Significance

**Understanding molecular and cellular mechanisms of rare genetic diseases provides invaluable insights into the human biology and pathology of both rare and related common diseases. Fibrous dysplasia (FD) is a mosaic disease resulting from postzygotic activating mutations of *GNAS*. The mouse models we created allowed us to precisely model FD by expressing the FD Gα$_s$ mutation under the control of its endogenous genetic locus. We found in our FD mouse models that up-regulated Wnt/β-catenin signaling resulted in impaired differentiation and proliferation of bone marrow stem cells, which in turn caused marrow fibrosis. Our work provides a solid new foundation for therapeutic development of FD and understanding the principles whereby Gα$_s$ signaling governs bone formation and maintenance and bone marrow stromal cell differentiation.**

Author contributions: S.K.K. and Y.Y. designed research; S.K.K., P.S.Y., G.E., D.Z.H., and R.X. performed research; S.K.K., P.S.Y., and Y.Y. analyzed data; and S.K.K., P.S.Y., and Y.Y. wrote the paper.

The authors declare no conflict of interest.

This article is a PNAS Direct Submission.



[1]To whom correspondence should be addressed. Email: yingzi_yang@hsdm.harvard.edu.

This article contains supporting information online at www.pnas.org/lookup/suppl/doi:10.1073/pnas.1714313114/-/DCSupplemental.

phenotypes. Furthermore, mosaic analysis showed that FD mutant *Gnas* expression in Sox9$^+$ BMSCs exhibits both cell-autonomous and non–cell-autonomous activities in causing FD phenotypes. Molecularly, as we have found in human FD bone previously, the FD mutant $G\alpha_s$ up-regulated Wnt/β-catenin signaling in bone and BMSCs, reduction of which significantly rescued FD phenotypes in *Gnas*$^{R201H}$ mice, providing important therapeutic insights.

## Results

**The *Gnas*$^{R201H}$ Mutation Is Embryonic Lethal.** Previously established mouse models have contributed to our current understanding of FD (13–15); however, due to the transgenic nature of the reported FD mouse lines and some inconsistent results obtained from these models, many outstanding questions remain unanswered. To further understand the critical roles of *Gnas* in multiple aspects of bone formation, maintenance, and resorption, including regulation of BMSCs as well as onset, progression, and cellular origins of FD, we have established a mouse line that allows conditional expression of mouse mutant $G\alpha_s$ containing a corresponding human FD mutation, R201H (4–6), from the endogenous mouse *Gnas* locus. This conditional KI *Gnas* allele [hereafter denoted *Gnas*$^{f(R201H)}$] was generated by homologous recombination in embryonic stem cells (Fig. S1*A*). The *Gnas* coding exon sequence is highly conserved between human and mouse (>90% sequence identity) both at nucleotide and amino acid levels (Fig. S2 *A* and *B*). The correctly targeted *Gnas*$^{f(R201H)}$ allele expressed mutant *Gnas*, which we denote as *Gnas*$^{R201H}$, only in the presence of *Cre* expression; otherwise, it expressed a wild-type *Gnas* containing the minigene cassette (Figs. S1*A* and S2*C*).

Mosaicism of the human FD GNAS R201H mutation suggested that *GNAS*$^{R201H}$ germ-line transmission may cause embryonic lethality. The *Gnas*$^{f(R201H)}$ allele we generated allowed us to test this directly by expressing *Gnas*$^{R201H}$ in the early epiblast [before embryonic day (E)6.5] using the *Sox2-Cre* line that expresses *Cre* in mouse oocytes (16). Indeed, all *Gnas*$^{f(R201H)/+}$; *Sox2-Cre* mutants with *Gnas*$^{R201H}$ heterozygous expression were found to be much smaller than wild-type littermate controls at E10.5 and dead some time between E12.5 and E15.5 (Fig. 1*A*). Expression of the mutant allele was confirmed by sequencing the *Gnas* cDNA made from whole embryos (Fig. S2*C*). Because $G\alpha_s$ signaling regulates both Wnt and Hedgehog (Hh) signaling (17, 18), we examined signaling activities of the Wnt and Hh pathways by whole-mount in situ hybridization as well as real-time quantitative PCR (qRT-PCR). Our results showed that while there was a significant up-regulation in the expression of *Tcf1* and *Axin2* (Fig. 1 *B* and *C*), which are Wnt/β-catenin target genes (19), expression of *Gli1* and *Ptch1* (Fig. 1 *D* and *E*), which are Hh signaling target genes (20–22), was down-regulated. *Shh* expression itself was not altered in the mutant embryos (Fig. S2*D*). Therefore, *Gnas*$^{R201H}$ expression in early embryos enhanced Wnt/β-catenin signaling, while it suppressed Hh signaling. The mutant embryos at E10.5 exhibited severe heart development retardation (Fig. S2*E*) as well as increased cell death and reduced cell proliferation in the entire embryo (Fig. S2 *F* and *G*). As Wnt/β-catenin and Hh signaling are two key signaling pathways required to regulate various aspects of early embryonic development (19, 23–26), it is likely that dysregulation of both by the activating R201H $G\alpha_s$ has caused embryonic lethality.

***Gnas*$^{R201H}$ Expression in Osteochondral Progenitor Cells Exhibits FD Features.** As FD-causing *GNAS* mutations are thought to occur at an early embryonic stage, we hypothesized that *Gnas*$^{R201H}$ expression in early mouse osteochondral progenitor cells should phenocopy human FD. To test our hypothesis, *Gnas*$^{f(R201H)}$ mice were crossed with the *Prrx1-Cre* line, in which *Cre* is expressed in early limb bud mesenchyme cells (27). All *Prrx1-Cre; Gnas*$^{f(R201H)/+}$ pups were born alive at Mendelian ratio and were readily distinguishable from wild-type littermates at birth due to their shorter limbs. The *Prrx1-Cre; Gnas*$^{f(R201H)/+}$ mice manifested marked shortening of the limbs with severe bone deformity (Fig. 2*A*) throughout their adulthood (Fig. S3 *A*, *B*, and *D*), while the *Gnas*$^{f(R201H)/+}$ littermate controls were normal and used as wild-type control in all analyses. Despite the short and misshapen limbs, bones in the trunk were normal and the mutant mice survived for more than 7 months with no sign of other gross sickness (Fig. S3 *C* and *D*). In *Prrx1-Cre; Gnas*$^{f(R201H)/+}$ mice, the bone marrow space was occupied by woven trabecular bone and there was no cortical bone (Fig. 2*B* and Fig. S3*D*). Histomorphometric analysis showed that the trabecular thickness and trabecular number were significantly increased, whereas trabecular spacing was decreased in mutant bone (Fig. S3 *E* and *F*).

Histological analysis further revealed abnormal architecture, structure, and mineral content of long bones in the *Prrx1-Cre; Gnas*$^{f(R201H)/+}$ mutant mice (Fig. 2 *C* and *D*). The growth plate cartilage was disorganized and expanded in the mutant compared with the control (Fig. S3*G*). The marrow cavity was much reduced and the marrow space was occupied by trabecular bone and fibrous tissue with an appearance of the characteristic Chinese writing pattern (Fig. 2*C*). Reduced mineralization in the mutant bones was shown by von Kossa staining, and the increased osteoid surface demonstrated poor mineralization of increased bone formation in the *Prrx1-Cre; Gnas*$^{f(R201H)/+}$ mutant mice (Fig. 2 *D* and *E*). Increased β-catenin protein levels were found in mutant long bones of postnatal day (P)6 pups (Fig. 2 *F* and *G*), supporting our previous findings in human FD bone (17). While poorly mineralized bone formation was increased, differentiation of osteoclasts from the *Prrx1-Cre*$^-$ hematopoietic lineage shown by tartrate-resistant acid phosphatase (TRAP) staining on the bone surface of the mutant mice was also increased (Fig. S3 *H* and *I*). This is a characteristic feature of human FD (28). In addition, *Rankl* expression was increased in *Prrx1-Cre; Gnas*$^{f(R201H)/+}$ mutant bone (Fig. S3*J*), suggesting that activating $G\alpha_s$ signaling in osteoblasts has up-regulated *Rankl* expression, as has been shown for osteoblast-derived parathyroid hormone-related peptide (PTHrP) that signals through $G\alpha_s$ and promotes *Rankl* expression directly (29, 30). All these phenotypes of *Prrx1-Cre; Gnas*$^{f(R201H)/+}$ mutant mice closely resemble those found in human FD. Therefore, embryonic expression of the activating R201H mutant $G\alpha_s$ in limb bud osteochondral progenitor cells recapitulated human FD phenotypes in adult long bones. It is important to note again that *Gnas*$^{R201H}$ heterozygous expression was sufficient to produce FD phenotypes in mice and that the phenotypes were the same in male or female mice regardless of whether *Gnas*$^{R201H}$ is provided maternally or paternally, as is the case in human FD (31).

**Progression of FD Phenotypes in *Prrx1-Cre; Gnas*$^{f(R201H)/+}$ Mutant Mice.** In humans, FD lesions start in embryonic development, progress during childhood, and remain static or sometimes improve in later stages of life (32). However, detailed tissue analysis of disease progression was not possible in human patients. The conditional *Prrx1-Cre; Gnas*$^{f(R201H)/+}$ mutant mice therefore allowed us to investigate the onset and progression of FD phenotypes to gain a better understanding of the natural history of FD disease.

Well-formed cortical bone, a marrow cavity with primary spongiosa next to the growth plate, and cartilaginous epiphyses can be seen in control mice starting from P0 (Fig. S4*A*), but the long bone of P0 *Prrx1-Cre; Gnas*$^{f(R201H)/+}$ mice showed no indication of bone formation (Fig. S4*A*). By P6, *Prrx1-Cre; Gnas*$^{f(R201H)/+}$ mice showed bone formation, but marrow space was occupied by osseous trabecular tissue and the growth plate was increased in length (Fig. S4*B*). At 3 wk of age, there was more bone formation in the *Prrx1-Cre; Gnas*$^{f(R201H)/+}$ mice with the same abnormalities as observed at P6: an irregular and thickened growth plate, lack of cortical bone, and expanded woven trabecular bone (Fig. S4*C*).

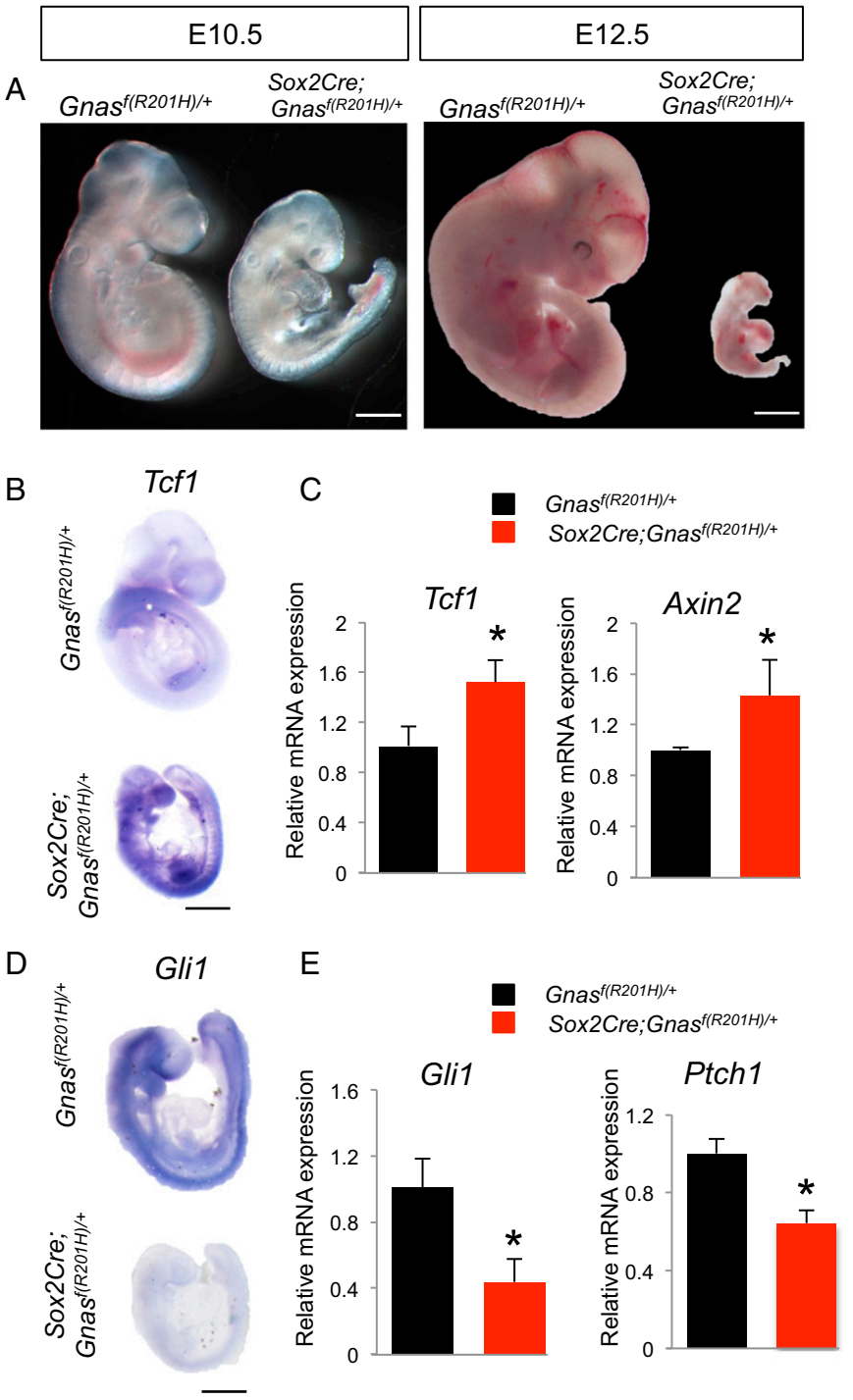


**Fig. 1.** Germ-line expression of *Gnas*$^{R201H}$ causes embryonic lethality. (*A*) Lateral view of E10.5 and E12.5 littermate embryos with the indicated genotypes. (*B* and *D*) Representative images of whole-mount in situ hybridization performed with E9.5 embryos. (*C* and *E*) qRT-PCR analysis of the indicated gene expression from RNA isolated from whole embryos at E9.5. *$P < 0.05$; data are presented as mean ± SD. (Scale bars, 100 mm.)

These phenotypes were also observed in 2- and 4-mo-old *Prrx1-Cre; Gnas*$^{f(R201H)/+}$ mice (Figs. S3*D* and S4*D*). Bone marrow fibrosis was observed from P6 onward.

The phenotypes of increased growth plate and delayed bone formation resembled those observed in mice in which either PTHrP or a constitutively active PTH/PTHrP receptor found in Jansen's metaphyseal chondrodysplasia (JMC) (33) was expressed in chondrocytes, which led to chondrodysplasia and delayed bone formation (34, 35). As the PTH/PTHrP receptor is coupled with $G\alpha_s$ (36), delayed bone formation and growth plate abnormalities in *Prrx1-Cre; Gnas*$^{f(R201H)/+}$ mice indicated that PTH/PTHrP signaling has been enhanced in the limb. Chondrocyte hypertrophy in long bone development is tightly regulated by a negative feedback loop formed by Indian Hedgehog (Ihh) and PTHrP (37–39), and enhanced PTHrP signaling delays chondrocyte hypertrophy (40, 41). To examine chondrocyte hypertrophy, we analyzed E15.5 and E18.5 embryonic cartilage in the limb both histologically and molecularly (Fig. S5). Marker expression of nonhypertrophic

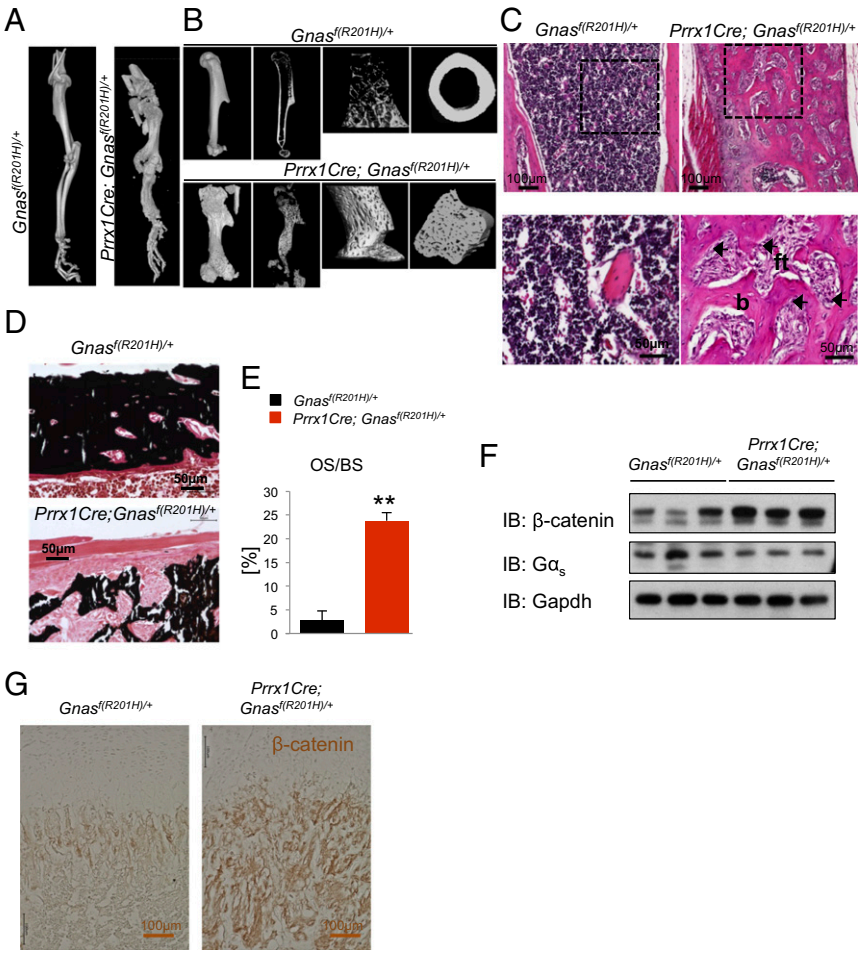


**Fig. 2.** *Prrx1-Cre; Gnas*$^{f(R201H)/+}$ mutant mice exhibit FD phenotypes. (*A* and *B*) Representative μCT scans of forelimbs from P21 mice with the indicated genotypes. Long bones were deformed in the mutant. Longitudinal and cross-sectional images of the humerus (*B*) showed that bone marrow space was occupied by trabecular bone in mutant mice. (*C*) Representative H&E staining of the trabecular region of P21 mouse humerus. Boxed regions are enlarged (*Bottom*); b, bone; ft, fibrous tissues. (*D*) von Kossa staining showing mineralization in humerus sections of P21 littermate control and mutant mice. (*E*) Quantification of mineralization in humerus from P21 mice as the percent of osteoid surface (OS) of bone surface (BS) ($n = 3$). (*F*) Western blot analysis for β-catenin and $G\alpha_s$ from the cell lysates of P6 humerus. IB, immunoblotting. (*G*) Immunohistochemistry of β-catenin on humerus sections of P6 littermate control and mutant mice. $^{**}P < 0.001$; data are presented as mean ± SD.

(*Col2*) (42, 43), prehypertrophic (*Ihh*) (38, 44), hypertrophic (*Col10*), and late hypertrophic chondrocytes (*Mmp13*) (45–47) was examined (Fig. S5*C*). In the mutant section, *Col2* expression was detected everywhere at the expense of *Ihh*, *Col10*, and *Mmp13* expression. In addition, delay of chondrocyte hypertrophy and the resulting delayed *Ihh* expression (Fig. S5*C*) caused delay in osteoblast differentiation in the mutant, shown by delayed osteoblast marker Osterix (Osx) expression (Fig. S5*D*). Taken together, $G\alpha_s$ activation delayed chondrocyte hypertrophy, which in turn delayed bone formation in embryos. Abnormal woven bone formation started postnatally and progressed rapidly with marrow fibrosis in *Prrx1-Cre; Gnas*$^{f(R201H)/+}$ mice. In addition, as a PTH/PTHrP receptor mutation was found in a few enchondroma patients and transgenic expression of one mutant *PTH/PTHrP receptor* led to enchondroma formation, supporting a role of the cAMP/PKA pathway in the development of enchondromas (48), some of the abnormal cartilage in older *Prrx1-Cre; Gnas*$^{f(R201H)/+}$ mice resembled enchondroma-like lesions in some FD patients (49, 50) (Fig. S4*D*, arrows).

***Gnas*$^{R201H}$ Expression Impairs Osteoblastic Differentiation of Bone Marrow Mesenchymal Stem Cells.** It has previously been shown that $G\alpha_s$ signaling plays a critical role in osteoblast differentiation from mesenchymal progenitor cells by modulating activities of the Wnt/β-catenin and Hh signaling pathways; both play fundamental roles in skeletal development, and defects in these signaling pathways cause skeletal diseases (18, 51, 52). In FD patients, there is extensive marrow fibrosis, and fibrotic cells in the marrow are arrested at early osteoblast differentiation stages (53, 54), suggesting that in adults, FD mutations cause aberrant osteoblast differentiation of BMSCs that contain stem cells. To test whether *Gnas*$^{R201H}$ expression in mouse BMSCs affects their osteogenic potential, we isolated BMSCs from *Gnas*$^{f(R201H)/+}$ mice and infected them with adenoviruses carrying Cre or GFP (Ad-Cre or Ad-GFP). Cre expression in BMSCs induced *Gnas*$^{R201H}$ expression and thus activated PKA, shown by increased CREB phosphorylation (55, 56) (Fig. 3*A*). The *Gnas*$^{R201H}$-expressing BMSCs cultured in osteogenic medium showed marked reduction in alkaline phosphatase (ALP) activity and mineralization (Fig. 3*B*). In addition, expression of osteogenic genes, such as *Osx* and *Osteocalcin* (*Ocn*), were significantly down-regulated (Fig. 3*C*). Importantly, *Gnas*$^{R201H}$ expression in BMSCs also reduced colony-forming units, suggesting that activated $G\alpha_s$ reduced stemness and/or proliferation of BMSCs (Fig. 3*D*). Furthermore, β-catenin protein levels were increased and expression of Wnt/β-catenin target genes *Axin2* and *Tcf1* were significantly up-regulated (Fig. 3 *E* and *F*) while Hh signaling was down-regulated in mutant

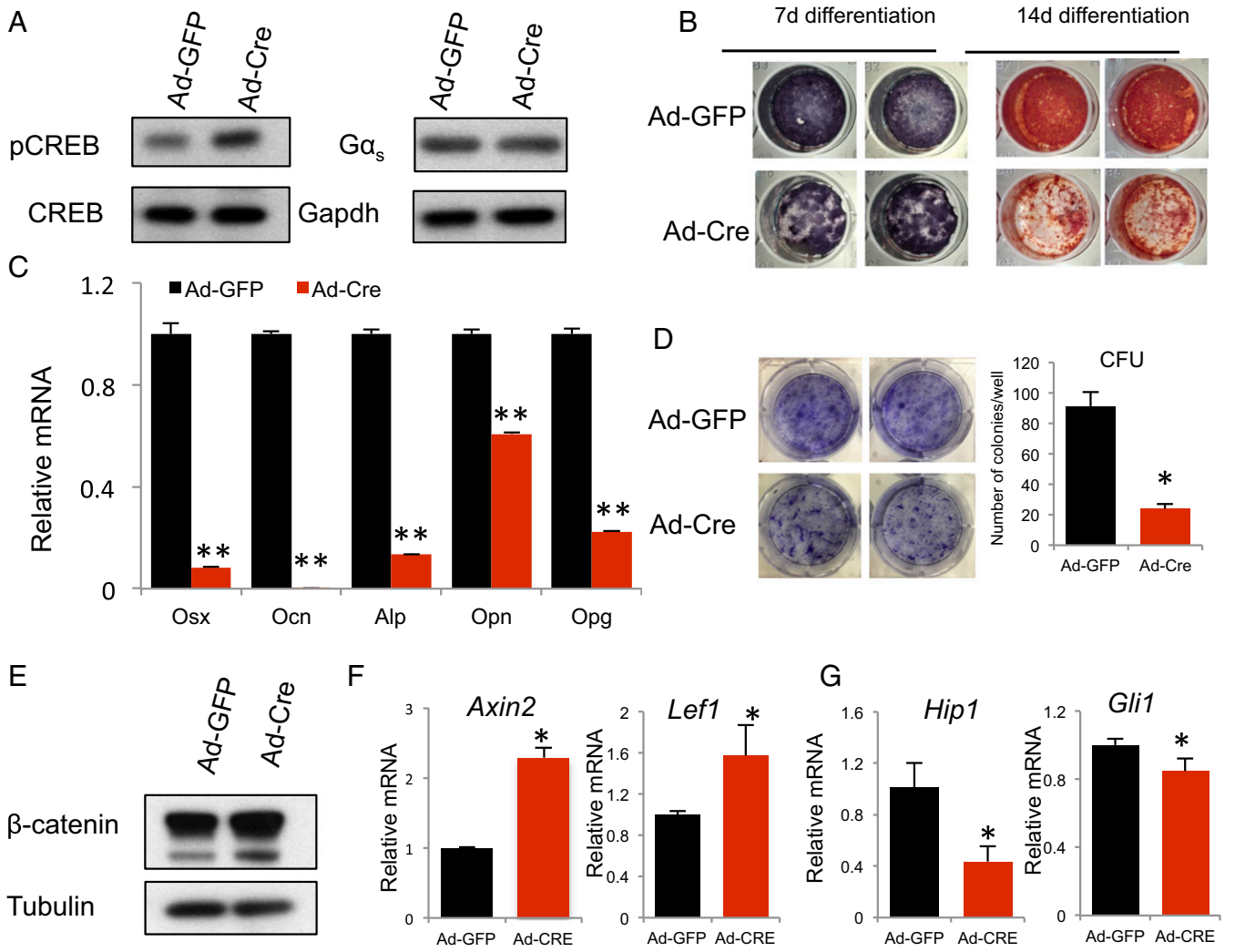


**Fig. 3.** *Gnas*$^{R201H}$ expression impairs osteoblastic differentiation of BMSCs. (*A*) Western blot analysis of phosphorylated CREB and Gα$_s$ in cell lysates of BMSCs 7 d after being transduced with Ad-Cre and Ad-GFP. (*B*) ALP and alizarin red staining of BMSCs after osteogenic differentiation for 7 and 14 d, respectively. (*C*) qRT-PCR analysis of osteogenic marker expression from the RNA isolated from BMSCs 7 d post differentiation after being transduced with Ad-Cre or Ad-GFP. (*D*) Colony-forming assay of BMSCs transduced with Ad-Cre or Ad-GFP. (*E*) Western blot analysis of β-catenin in BMSCs 7 d after being transduced with Ad-Cre or Ad-GFP. (*F* and *G*) qRT-PCR analysis of signaling target genes of the Wnt (*Axin2* and *Lef1*) and Hedgehog (*Hip1* and *Gli1*) pathways from RNA isolated from BMSCs 7 d after being transduced with Ad-Cre and Ad-GFP. **P* < 0.05, ***P* < 0.001; data are presented as mean ± SD.

BMSCs (Fig. 3*G*), consistent with our previous findings (17, 18, 51) that activated Gα$_s$ promotes Wnt/β-catenin signaling and inhibits Hh signaling.

**Mosaic Analysis Reveals Non–Cell-Autonomous Roles of the Gα$_s$ FD Mutation in BMSCs.** As FD in humans is caused by somatic mosaicism of Gα$_s$ mutations, to model this disease more accurately, we created a mosaic state of the *Gnas*$^{R201H}$ mutation in vivo in bone by crossing the *Gnas*$^{f(R201H)}$ line with *Sox9-CreER; Rosa26Td-Tomato* mice to generate *Gnas*$^{f(R201H)}$*; Sox9-CreER; Rosa26Td-Tomato* mice. The *Sox9-CreER* line was chosen, as it has been shown to be expressed in BMSCs after birth apart from its expression in chondrocytes (57). Tamoxifen (TM)-injected mosaic mutant mice exhibited increased bone volume as well as trabecular number and thickness and displayed an irregular growth plate architecture (Fig. S6 *A* and *B*) similar to, but less severe than, the phenotypes of *Prrx1-Cre; Gnas*$^{f(R201H)}$ mice. Tdtomato marked the *Gnas*$^{R201H}$ mutant cells, and increased CREB phosphorylation was found in Tdtomato$^+$ cells, confirming Gα$_s$ activation (Fig. S6*C*). Interestingly, Osx$^+$ osteoprogenitor cells were increased in the Tdtomato$^+$ population while Osteopontin (Opn$^+$) cells were reduced (Fig. 4 *A*, *A′*, *B*, and *B′*), indicating that *Gnas*$^{R201H}$ expression promotes osteoblast differentiation from BMSCs but inhibits osteoblast maturation in vivo. Consistent with findings in *Prrx1-Cre; Gnas*$^{f(R201H)}$ mice, β-catenin expression was increased in the Tdtomato$^+$ population (Fig. S6*E*).

The growth plate was very disorganized in the TM-injected *Sox9-CreER; Rosa26Td-Tomato; Gnas*$^{f(R201H)}$ mutant mice. As chondrocyte hypertrophy is synchronized in wild-type mice, we asked whether disorganization of the mutant growth plate was caused by asynchronous hypertrophy due to mosaic expression of *Gnas*$^{R201H}$. Indeed, Col10 immunostaining showed that the *Gnas*$^{R201H}$-expressing Tdtomato$^+$ chondrocyte column was much increased in length compared with the wild-type Tdtomato$^+$ chondrocyte column or Tdtomato$^-$ one (Fig. 4 *C*–*C″*), demonstrating that *Gnas*$^{R201H}$ expression significantly delayed chondrocyte hypertrophy cell autonomously.

As bone marrow fibrosis is a prominent feature of FD, we also found extensive fibrotic tissue in bone marrow of TM-injected *Gnas*$^{f(R201H)}$*; Sox9-CreER; Rosa26Td-Tomato* mutant

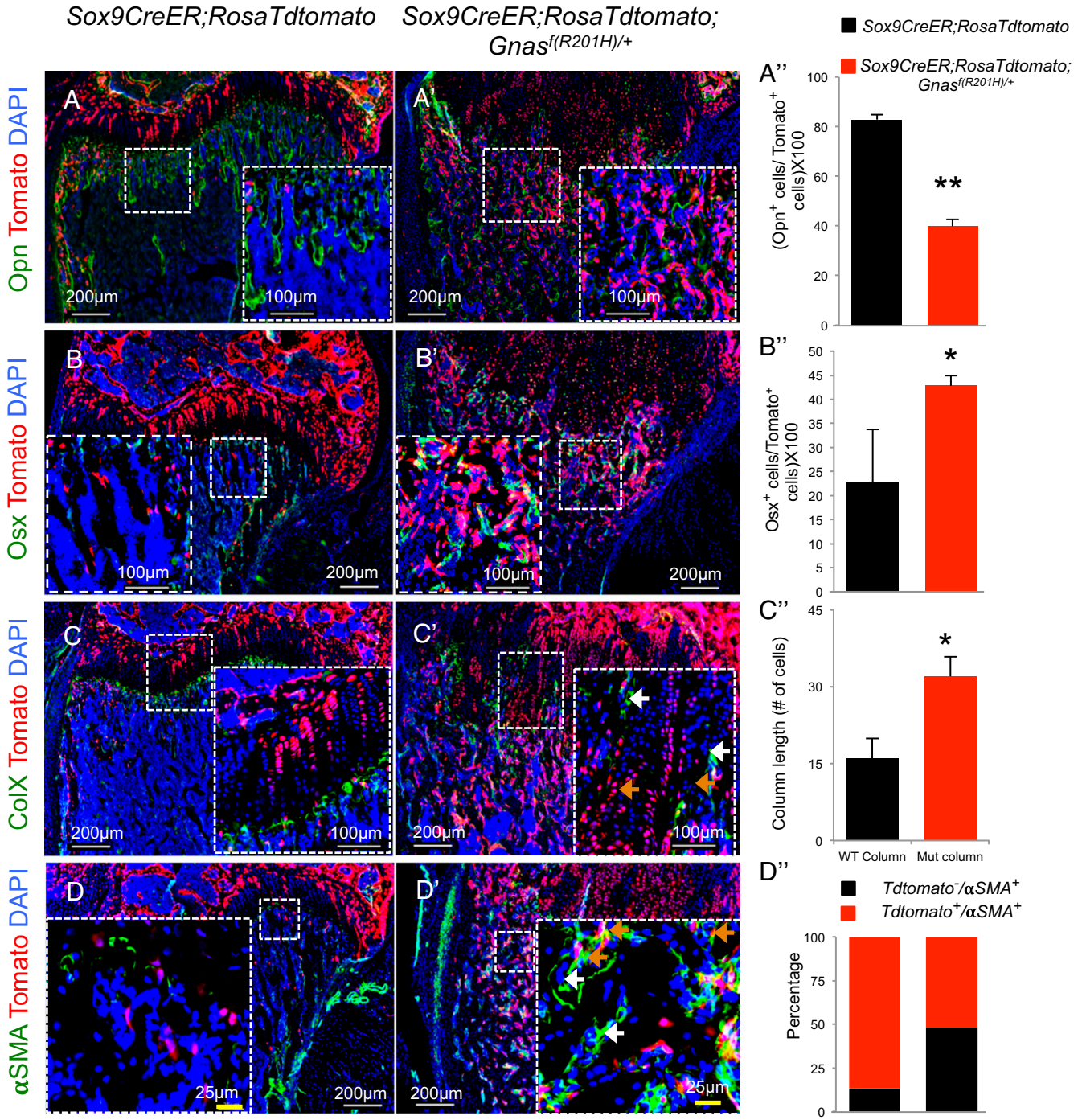


**Fig. 4.** Mosaic expression of *Gnas*$^{R201H}$ causes enhanced bone fibrosis but reduced bone maturation. Immunostaining (*A–D* and *A′–D′*) and quantification (*A″–D″*) of marker expression as indicated in TdTomato-labeled mutant [*Sox9-CreER; Rosa26TdTomato; Gnas*$^{f(R201H)}$] in wild-type (*Sox9-CreER; Rosa26TdTomato*) cells. TM was injected at P5 and the humerus was sectioned at P21 for analysis. *$P < 0.05$, **$P < 0.001$; data are presented as mean ± SD. Opn$^+$ and Osx$^+$ cells refer to Opn$^+$; TdTomato$^+$ and Osx$^+$; TdTomato$^+$ double-positive cells.

mice compared with the TM-injected wild-type control (Fig. S6*B*). When analyzed with a fibrosis marker, αSMA (58), there was an increase of αSMA$^+$ cells in the mutant mice (Fig. 4 *D–D′*). This was further confirmed by much increased αSMA expression in *Gnas*$^{R201H}$-expressing BMSCs (Fig. S6*D*). Interestingly, many of the αSMA$^+$ cells were Tdtomato$^-$, suggesting that they were wild-type cells with no *Gnas*$^{R201H}$ expression (Fig. 4*D′*). In addition, these αSMA$^+$; Tdtomato$^-$ cells were not associated with CD31$^+$ endothelial cells (Fig. S6 *F* and *G*), indicating they were not smooth muscle cells associated with blood vessels. Therefore, *Gnas*$^{R201H}$ expression in BMSCs also caused FD, and mosaic analysis allowed uncovering non–cell-autonomous activities of *Gnas*$^{R201H}$ in bone marrow fibrosis.

**Wnt/β-Catenin Signaling Plays a Key Role in FD Pathogenesis.** As *Prrx1-Cre* and *Sox9-CreER* are also expressed in chondrocytes, to investigate whether *Gnas*$^{R201H}$ expression in early osteoblast progenitors would lead to FD, we crossed the *Gnas*$^{f(R201H)}$ line

with the *Osx-GFP::Cre* line, a tetracycline responsive element (tetO)-controlled *GFP::Cre* fusion gene expression driven by the *Osx* promoter (59). To our surprise, mutant mice died immediately after birth, possibly due to general bone defects throughout the body. To get around this, we suppressed *GFP::Cre* expression by feeding pregnant female mice with doxycycline in water starting at E11.5 until birth. The pups were born with grossly normal morphology but, at weaning, mutant mice showed strong FD phenotypes, though less severe than the *Prrx1-Cre; Gnas*$^{f(R201H)}$ mice (Fig. 5 *A* and *B*). As we found that Wnt/β-catenin signaling was highly up-regulated in both *Prrx1-Cre*– and *Sox9-CreER*–driven mutants, we decided to genetically down-regulate it in this less severe FD model to see if reducing Wnt/β-catenin signaling can rescue the FD phenotype by generating *Osx-GFP::Cre; Gnas*$^{f(R201H)}$*; Lrp6*$^{c/+}$ mice. Lrp6 is a Wnt coreceptor that transmits canonical Wnt/β-catenin signaling (60). Interestingly, removing one

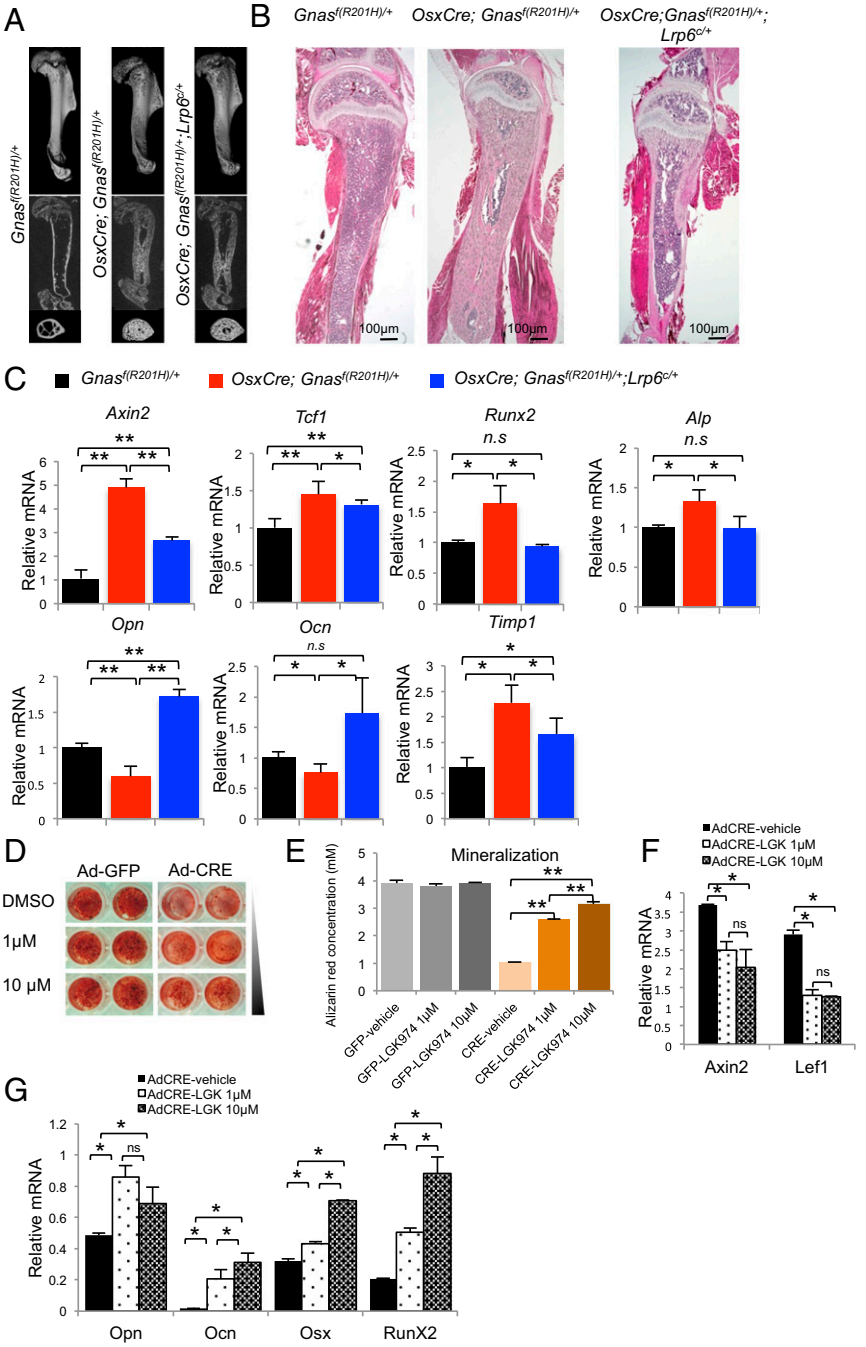


**Fig. 5.** Up-regulated Wnt/β-catenin signaling plays a key role in FD. (*A*) Representative μCT scans of the humerus of littermate control [*Gnas*$^{f(R201H)/+}$] and *OsxCre; Gnas*$^{f(R201H)/+}$ and *OsxCre; Gnas*$^{f(R201H)/+}$*; Lrp6*$^{C/+}$ mutant mice. Sagittal and transverse section views of humerus are also shown. (*B*) H&E staining of humerus sections from P21 mice of the indicated genotypes. (*C*) qRT-PCR analysis of humerus bones from mice with the indicated genotypes. (*D*) Alizarin red staining of BMSCs transduced with Ad-Cre and Ad-GFP viruses 7 d after osteogenic differentiation. At day 0 of osteogenic differentiation, BMSCs were treated with DMSO or LGK-974, a small molecule that inhibits Wnt secretion. (*E*) Alizarin red staining was quantified. (*F* and *G*) qRT-PCR analysis of gene expression in BMSCs at day 7 post differentiation. $*P < 0.05$, $**P < 0.001$; ns, not significant; data are presented as mean ± SD.

*Lrp6* copy in *Osx-GFP::Cre; Gnas*$^{f(R201H)}$ mutant mice resulted in significant rescue of FD phenotypes. Microcomputed tomography (μCT) as well as histological analysis showed obvious rescue of bone marrow space and cortical bone as well as reduction of bone marrow fibrosis (Fig. 5 *A* and *B*). Wnt/β-catenin target gene expression was reduced by *Lrp6* removal (Fig. 5*C*). Furthermore, expression of early osteoblast differentiation markers such as *Runx2* and *Alp* was reduced, while expression of mature osteoblast markers *Ocn* and *Opn* was increased and fibrosis marker *Timp1* was decreased in the rescued mutants (Fig. 5*C*). Therefore, up-regulated canonical Wnt/β-catenin signaling plays a key role in mediating the effects of *Gnas*$^{f(R201H)}$ expression in FD. Osteoclast differentiation was not altered by removing *Lrp6* (Fig. S7). To further test the therapeutic value of small-molecule inhibitors of Wnt/β-catenin signaling in improving bone mineralization inhibited by *Gnas*$^{R201H}$, we treated *Gnas*$^{R201H}$-expressing BMSCs at the beginning of osteogenic differentiation with LGK-974, a potent small-molecule inhibitor of Wnt secretion (61). LGK-974 treatment dose dependently improved mineralization in *Gnas*$^{R201H}$ mutant BMSCs (Fig. 5 *D* and *E*), which was confirmed by reduced Wnt signaling and increased osteogenic marker expression (Fig. 5 *F* and *G*). Taken together, both in vivo and in vitro experiments demonstrate that up-regulated canonical Wnt/β-catenin signaling mediates the function of *Gnas*$^{R201H}$ in causing FD, and that Wnt/β-catenin signaling may be a critical therapeutic target for treating FD.

## Discussion

Here we report the generation of a mouse model that allows the closest possible modeling of FD bone disease, a skeletal disorder originally described in 1942 (62). The conditional knockin approach allowed expression of *Gnas*$^{R201H}$ corresponding to the human FD mutant from the *Gnas* locus with spatial and temporal control. This model can be used to study not only FD but also MAS, which has severe symptoms outside of the skeletal system. Germ-line expression of *Gnas*$^{R201H}$ caused embryonic lethality, but Cre-induced *Gnas*$^{R201H}$ expression in osteochondral progenitor cells, early osteoblast cells, or sporadically in postnatal BMSCs led to typical FD phenotypes. Embryonic lethality due to germ-line *Gnas*$^{R201H}$ expression confirmed the longstanding hypothesis postulated by Happle that the disease genotype would be lethal if germ line-transmitted, and is only able to survive through mosaicism (12). Successful development of the *Gnas*$^{f(R201H)}$ line has opened a door to elucidating many still poorly understood aspects of FD and MAS and to designing and testing novel FD treatment strategies.

Our finding, though consistent with the human FD etiology that is linked to missense activating *GNAS* mutations that occur after fertilization in somatic cells (5, 63), is in contrast with a previous finding in a transgenic model in which the human FD mutant transgene could survive through germ-line transmission (13). This is likely due to the transgenic nature of the previous model in which an artificial promoter was driving the mutant *GNAS* cDNA expression from a heterologous genomic locus, highlighting the necessity to express the FD mutant from the endogenous *Gnas* locus to precisely model the disease. Several other animal models have been generated in the past that contributed to our current understanding of FD. These models, though insightful in certain ways, are limited in others by their transgenic and interspecies tissue transplantation nature, which does not change the $G\alpha_s$ expressed from its endogenous locus as in FD human patients. Furthermore, these models could not be used to study other associated phenotypes found in MAS, where $G\alpha_s$ activation occurs outside of the skeleton.

Interestingly, we found that induced *Gnas*$^{R201H}$ expression in osteochondral progenitor cells resulted in much delayed chondrocyte hypertrophy, a thickened growth plate, and a condition similar to enchondroma (Fig. S4*D*). It is well-recognized that an FD lesion may contain cartilage, though the amount is quite variable. Jaffe and Lichtenstein (64) in their original article on FD recognized that cartilage was "an integral part of the dysplastic process"; FD case reports have shown that multifocal FD has been found together with enchondroma-like areas in conditions of fibrocartilaginous dysplasia (FCD) (65, 66). The animal models we have generated provided invaluable insight and tools in understanding FD and FCD. The PTH/PTHrP receptor couples to $G\alpha_s$ and $G\alpha_q$/11 (67–69). Patients with JMC (characterized by short-limbed dwarfism, severe growth plate abnormalities, and hypercalcemia) and also a few patients with enchondroma alone (48) carry activating mutations in the PTH/PTHrP receptor that cause constitutive receptor activation (33, 70). Delayed chondrocyte hypertrophy and FCD-like lesions in our FD models resemble those caused by activated PTH/PTHrP receptor. It is interesting to observe that chondrocyte hypertrophy eventually occurred in *Gnas*$^{f(R201H)}$; *Prrx1-Cre* newborn pups (Fig. S4). As other signaling pathways can also regulate chondrocyte hypertrophy, it is possible that postnatally, the relative contribution of the PTH/PTHrP receptor in regulating chondrocyte hypertrophy is reduced.

The cellular origin of FD has remained largely unknown. Our data demonstrate that expression of FD mutation in early osteochondral progenitor cells or osteoblast lineage cells, or BMSCs, can establish similar human FD phenotypes. In all these FD models, consistent with our previous finding in human tissues (17), Wnt/β-catenin signaling was up-regulated; this is critical for FD phenotypes, as removal of one *Lrp6* gene copy resulted in significant rescue of FD phenotypes, demonstrating that activated Wnt/β-catenin signaling is a key mechanism that induces FD. The function of Wnt signaling in bone formation has been shown to be dose- and stage-dependent. Sustained activation of Wnt/β-catenin signaling in mesenchymal progenitor cells and osteoblast lineages results in reduced mineralization and bone formation (ref. 17 and references therein). Both in vivo genetic rescue and in vitro chemical treatment showed that inhibition of Wnt/β-catenin signaling reduced FD phenotypes by promoting osteoblast maturation and reducing bone marrow fibrosis. Therefore, Wnt/β-catenin signaling inhibitors such as LGK-974 could be repurposed to treat FD, and our FD models are well-suited to test potential treatments for FD and McCune–Albright syndrome.

## Materials and Methods

**Mouse.** Animal care and experiments were performed in accordance with the Institutional Animal Care and Use Committee (IACUC) guidelines at the National Institutes of Health and the Harvard Medical School.

**Immunohistochemistry and Western Blotting.** Immunohistochemistry was performed according to previously described methods (18). Western blotting was performed using standard techniques. Antibody information is provided in *Supporting Information*.

**RNA in Situ Hybridization.** RNA in situ hybridization was performed using DIG-labeled antisense RNA probes as described before (71).

**BMSC Isolation and Osteogenic Differentiation.** BMSCs were isolated by flushing the bone marrow cavity of 6-wk-old mice and plating cells in alpha-MEM, 20% FBS, 100 U/mL penicillin, and 100 μg/mL streptomycin. Equal numbers of cells were then seeded in 12-well plates and infected with Ad-Cre or Ad-GFP before confluence. Cells were switched to osteogenic medium (17, 18) after confluence for the indicated time before analysis.

**Adenovirus Cell Culture Treatment.** The Cre and GFP adenoviruses were made by SAIC-Frederick (~$1 \times 10^{10}$ pfu/mL) and diluted 1:500 for infection.

**Statistical Analysis.** Statistical significance was tested by two-tailed Student's *t* test between two groups. $P < 0.05$ was considered significant. Data are presented as mean ± SD unless otherwise indicated.

**ACKNOWLEDGMENTS.** We thank members of the Y.Y. laboratory for constructive discussions, and the Harvard School of Dental Medicine (HSDM) μCT core and Center for Skeletal Research at Massachusetts General Hospital for μCT scanning. This study was supported by NIH Grants R01DE025866 from

National Institute of Dental and Craniofacial Research and R01AR070877 from National Institute of Arthritis and Musculoskeletal and Skin Diseases, the intramural research program of National Human Genome Research Institute, and the HSDM Dean's Scholar fellowship (to S.K.K.).


1. Riminucci M, et al. (1999) The histopathology of fibrous dysplasia of bone in patients with activating mutations of the Gs alpha gene: Site-specific patterns and recurrent histological hallmarks. *J Pathol* 187:249–258.
2. Riminucci M, et al. (1997) Fibrous dysplasia of bone in the McCune-Albright syndrome: Abnormalities in bone formation. *Am J Pathol* 151:1587–1600.
3. Robinson C, Collins MT, Boyce AM (2016) Fibrous dysplasia/McCune-Albright syndrome: Clinical and translational perspectives. *Curr Osteoporos Rep* 14:178–186.
4. Shenker A, Weinstein LS, Sweet DE, Spiegel AM (1994) An activating Gs alpha mutation is present in fibrous dysplasia of bone in the McCune-Albright syndrome. *J Clin Endocrinol Metab* 79:750–755.
5. Weinstein LS, et al. (1991) Activating mutations of the stimulatory G protein in the McCune-Albright syndrome. *N Engl J Med* 325:1688–1695.
6. Schwindinger WF, Francomano CA, Levine MA (1992) Identification of a mutation in the gene encoding the alpha subunit of the stimulatory G protein of adenylyl cyclase in McCune-Albright syndrome. *Proc Natl Acad Sci USA* 89:5152–5156.
7. Lania A, et al. (1998) Constitutively active Gs alpha is associated with an increased phosphodiesterase activity in human growth hormone-secreting adenomas. *J Clin Endocrinol Metab* 83:1624–1628.
8. Boyce AM, Collins MT (1993) Fibrous dysplasia/McCune-Albright syndrome. *GeneReviews*, eds Adam MP, et al. (Univ of Washington, Seattle).
9. Albright F, Butler AM, Hampton AO, Smith P (1937) Syndrome characterized by osteitis fibrosa disseminata, areas of pigmentation and endocrine dysfunction, with precocious puberty in females Report of 5 cases. *N Engl J Med* 216:727–746.
10. Shenker A, et al. (1993) Severe endocrine and nonendocrine manifestations of the McCune-Albright syndrome associated with activating mutations of stimulatory G protein GS. *J Pediatr* 123:509–518.
11. Bianco P, et al. (1998) Reproduction of human fibrous dysplasia of bone in immunocompromised mice by transplanted mosaics of normal and Gsalpha-mutated skeletal progenitor cells. *J Clin Invest* 101:1737–1744.
12. Happle R (1986) The McCune-Albright syndrome: A lethal gene surviving by mosaicism. *Clin Genet* 29:321–324.
13. Saggio I, et al. (2014) Constitutive expression of Gsα(R201C) in mice produces a heritable, direct replica of human fibrous dysplasia bone pathology and demonstrates its natural history. *J Bone Miner Res* 29:2357–2368.
14. Remoli C, et al. (2015) Osteoblast-specific expression of the fibrous dysplasia (FD)-causing mutation Gsα(R201C) produces a high bone mass phenotype but does not reproduce FD in the mouse. *J Bone Miner Res* 30:1030–1043.
15. Hsiao EC, et al. (2008) Osteoblast expression of an engineered Gs-coupled receptor dramatically increases bone mass. *Proc Natl Acad Sci USA* 105:1209–1214.
16. Hayashi S, Lewis P, Pevny L, McMahon AP (2002) Efficient gene modulation in mouse epiblast using a Sox2Cre transgenic mouse strain. *Mech Dev* 119(Suppl 1):S97–S101.
17. Regard JB, et al. (2011) Wnt/β-catenin signaling is differentially regulated by Gα proteins and contributes to fibrous dysplasia. *Proc Natl Acad Sci USA* 108: 20101–20106.
18. Regard JB, et al. (2013) Activation of Hedgehog signaling by loss of GNAS causes heterotopic ossification. *Nat Med* 19:1505–1512.
19. Clevers H (2006) Wnt/beta-catenin signaling in development and disease. *Cell* 127: 469–480.
20. Huangfu D, Anderson KV (2006) Signaling from Smo to Ci/Gli: Conservation and divergence of Hedgehog pathways from *Drosophila* to vertebrates. *Development* 133: 3–14.
21. Bai CB, Auerbach W, Lee JS, Stephen D, Joyner AL (2002) Gli2, but not Gli1, is required for initial Shh signaling and ectopic activation of the Shh pathway. *Development* 129: 4753–4761.
22. Goodrich LV, Johnson RL, Milenkovic L, McMahon JA, Scott MP (1996) Conservation of the hedgehog/patched signaling pathway from flies to mice: Induction of a mouse patched gene by Hedgehog. *Genes Dev* 10:301–312.
23. van Amerongen R, Nusse R (2009) Towards an integrated view of Wnt signaling in development. *Development* 136:3205–3214.
24. Yang Y (2012) Wnt signaling in development and disease. *Cell Biosci* 2:14.
25. Varjosalo M, Taipale J (2008) Hedgehog: Functions and mechanisms. *Genes Dev* 22: 2454–2472.
26. Chiang C, et al. (1996) Cyclopia and defective axial patterning in mice lacking Sonic hedgehog gene function. *Nature* 383:407–413.
27. Logan M, et al. (2002) Expression of Cre recombinase in the developing mouse limb bud driven by a Prxl enhancer. *Genesis* 33:77–80.
28. Riminucci M, et al. (2003) Osteoclastogenesis in fibrous dysplasia of bone: In situ and in vitro analysis of IL-6 expression. *Bone* 33:434–442.
29. Martin TJ (2005) Osteoblast-derived PTHrP is a physiological regulator of bone formation. *J Clin Invest* 115:2322–2324.
30. Mak KK, et al. (2008) Hedgehog signaling in mature osteoblasts regulates bone formation and resorption by controlling PTHrP and RANKL expression. *Dev Cell* 14: 674–688.
31. DiCaprio MR, Enneking WF (2005) Fibrous dysplasia. Pathophysiology, evaluation, and treatment. *J Bone Joint Surg Am* 87:1848–1864.
32. Hart ES, et al. (2007) Onset, progression, and plateau of skeletal lesions in fibrous dysplasia and the relationship to functional outcome. *J Bone Miner Res* 22:1468–1474.
33. Schipani E, Kruse K, Jüppner H (1995) A constitutively active mutant PTH-PTHrP receptor in Jansen-type metaphyseal chondrodysplasia. *Science* 268:98–100.
34. Weir EC, et al. (1996) Targeted overexpression of parathyroid hormone-related peptide in chondrocytes causes chondrodysplasia and delayed endochondral bone formation. *Proc Natl Acad Sci USA* 93:10240–10245.
35. Schipani E, et al. (1997) Targeted expression of constitutively active receptors for parathyroid hormone and parathyroid hormone-related peptide delays endochondral bone formation and rescues mice that lack parathyroid hormone-related peptide. *Proc Natl Acad Sci USA* 94:13689–13694.
36. Jüppner H, et al. (1991) A G protein-linked receptor for parathyroid hormone and parathyroid hormone-related peptide. *Science* 254:1024–1026.
37. Karp SJ, et al. (2000) Indian hedgehog coordinates endochondral bone growth and morphogenesis via parathyroid hormone related-protein-dependent and -independent pathways. *Development* 127:543–548.
38. Vortkamp A, et al. (1996) Regulation of rate of cartilage differentiation by Indian hedgehog and PTH-related protein. *Science* 273:613–622.
39. Chung UI, Schipani E, McMahon AP, Kronenberg HM (2001) Indian hedgehog couples chondrogenesis to osteogenesis in endochondral bone development. *J Clin Invest* 107: 295–304.
40. Chung UI, Lanske B, Lee K, Li E, Kronenberg H (1998) The parathyroid hormone/parathyroid hormone-related peptide receptor coordinates endochondral bone development by directly controlling chondrocyte differentiation. *Proc Natl Acad Sci USA* 95:13030–13035.
41. Lanske B, et al. (1996) PTH/PTHrP receptor in early development and Indian hedgehog-regulated bone growth. *Science* 273:663–666.
42. Ng LJ, Tam PP, Cheah KS (1993) Preferential expression of alternatively spliced mRNAs encoding type II procollagen with a cysteine-rich amino-propeptide in differentiating cartilage and nonchondrogenic tissues during early mouse development. *Dev Biol* 159:403–417.
43. Sandell LJ, Morris N, Robbins JR, Goldring MB (1991) Alternatively spliced type II procollagen mRNAs define distinct populations of cells during vertebral development: Differential expression of the amino-propeptide. *J Cell Biol* 114: 1307–1319.
44. Kronenberg HM (2003) Developmental regulation of the growth plate. *Nature* 423: 332–336.
45. Mattot V, et al. (1995) Expression of interstitial collagenase is restricted to skeletal tissue during mouse embryogenesis. *J Cell Sci* 108:529–535.
46. Yoshida CA, et al. (2004) Runx2 and Runx3 are essential for chondrocyte maturation, and Runx2 regulates limb growth through induction of Indian hedgehog. *Genes Dev* 18:952–963.
47. Linsenmayer TF, et al. (1991) Collagen types IX and X in the developing chick tibiotarsus: Analyses of mRNAs and proteins. *Development* 111:191–196.
48. Hopyan S, et al. (2002) A mutant PTH/PTHrP type I receptor in enchondromatosis. *Nat Genet* 30:306–310.
49. Kalifa G, Adamsbaum C, Job-Deslande C, Dubousset J (1993) Fibrodysplasia ossificans progressiva and synovial chondromatosis. *Pediatr Radiol* 23:91–93.
50. Clauser L, Marchetti C, Piccione M, Bertoni F (1996) Craniofacial fibrous dysplasia and Ollier's disease: Combined transfrontal and transfacial resection using the nasal-cheek flap. *J Craniofac Surg* 7:140–144.
51. Day TF, Guo X, Garrett-Beal L, Yang Y (2005) Wnt/beta-catenin signaling in mesenchymal progenitors controls osteoblast and chondrocyte differentiation during vertebrate skeletogenesis. *Dev Cell* 8:739–750.
52. Regard JB, Zhong Z, Williams BO, Yang Y (2012) Wnt signaling in bone development and disease: Making stronger bone with Wnts. *Cold Spring Harb Perspect Biol* 4: a007997.
53. Marie PJ, de Pollak C, Chanson P, Lomri A (1997) Increased proliferation of osteoblastic cells expressing the activating Gs alpha mutation in monostotic and polyostotic fibrous dysplasia. *Am J Pathol* 150:1059–1069.
54. Riminucci M, Robey PG, Saggio I, Bianco P (2010) Skeletal progenitors and the GNAS gene: Fibrous dysplasia of bone read through stem cells. *J Mol Endocrinol* 45:355–364.
55. Yamamoto KK, Gonzalez GA, Biggs WH, III, Montminy MR (1988) Phosphorylation-induced binding and transcriptional efficacy of nuclear factor CREB. *Nature* 334: 494–498.
56. Bullock BP, Habener JF (1998) Phosphorylation of the cAMP response element binding protein CREB by cAMP-dependent protein kinase A and glycogen synthase kinase-3 alters DNA-binding affinity, conformation, and increases net charge. *Biochemistry* 37:3795–3809.
57. Ono N, Ono W, Nagasawa T, Kronenberg HM (2014) A subset of chondrogenic cells provides early mesenchymal progenitors in growing bones. *Nat Cell Biol* 16: 1157–1167.
58. Meng F, et al. (2012) Interleukin-17 signaling in inflammatory, Kupffer cells, and hepatic stellate cells exacerbates liver fibrosis in mice. *Gastroenterology* 143:765–776.e3.
59. Rodda SJ, McMahon AP (2006) Distinct roles for Hedgehog and canonical Wnt signaling in specification, differentiation and maintenance of osteoblast progenitors. *Development* 133:3231–3244.
60. Pinson KI, Brennan J, Monkley S, Avery BJ, Skarnes WC (2000) An LDL-receptor-related protein mediates Wnt signalling in mice. *Nature* 407:535–538.
61. Tammela T, et al. (2017) A Wnt-producing niche drives proliferative potential and progression in lung adenocarcinoma. *Nature* 545:355–359.
62. Lichtenstein LJ (1942) Fibrous dysplasia of bone. *Arch Pathol (Chic)* 33:777–816.

63. Weinstein LS, Chen M, Liu J (2002) Gs(alpha) mutations and imprinting defects in human disease. *Ann N Y Acad Sci* 968:173–197.
64. Jaffe HL, Lichtenstein L (1942) Benign chondroblastoma of bone: A reinterpretation of the so-called calcifying or chondromatous giant cell tumor. *Am J Pathol* 18: 969–991.
65. Vargas-Gonzalez R, Sanchez-Sosa S (2006) Fibrocartilaginous dysplasia (fibrous dysplasia with extensive cartilaginous differentiation). *Pathol Oncol Res* 12: 111–114.
66. Monappa V, Kudva R (2007) Multifocal fibrous dysplasia with enchondroma-like areas: Fibrocartilaginous dysplasia. *Internet J Pathol* 7:1–6.
67. Gardella TJ, Jüppner H (2001) Molecular properties of the PTH/PTHrP receptor. *Trends Endocrinol Metab* 12:210–217.
68. Bringhurst FR, et al. (1993) Cloned, stably expressed parathyroid hormone (PTH)/PTH-related peptide receptors activate multiple messenger signals and biological responses in LLC-PK1 kidney cells. *Endocrinology* 132:2090–2098.
69. Iida-Klein A, et al. (1997) Mutations in the second cytoplasmic loop of the rat parathyroid hormone (PTH)/PTH-related protein receptor result in selective loss of PTH-stimulated phospholipase C activity. *J Biol Chem* 272:6882–6889.
70. Schipani E, et al. (1999) A novel parathyroid hormone (PTH)/PTH-related peptide receptor mutation in Jansen's metaphyseal chondrodysplasia. *J Clin Endocrinol Metab* 84:3052–3057.
71. Prashar P, Yadav PS, Samarjeet F, Bandyopadhyay A (2014) Microarray meta-analysis identifies evolutionarily conserved BMP signaling targets in developing long bones. *Dev Biol* 389:192–207.